

Comparing Electrical Performance of Zn-Cu Flat Stacked and Rolled Galvanic Cells

Manas Srinivas, Emily Sewell, Lucas Sidney, Jacinta Wilkin, Bryan Law, Jordan Kambanis, Masoomeh Asghar Nejad-Laskoukalayeh, Benedict Tai, David Alam, Thomas Whittle, Gobinath Rajarathnam

School of Chemical & Biomolecular Engineering

E-mail:

Received xxxxxx

Accepted for publication xxxxxx

Published xxxxxx

Graphical Abstract

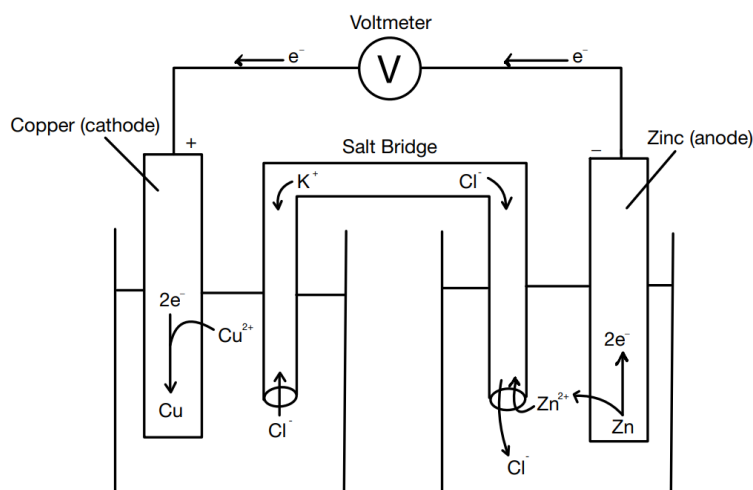


Figure 1. A standard zinc-copper galvanic cell

Abstract

Galvanic cells generate electricity from spontaneous redox reactions and are applied by chemical engineers in areas such as corrosion control and electroplating. This study investigates the electrochemical performance of zinc-copper (Zn-Cu) galvanic cells in flat-stacked and rolled configurations, isolating the influence of configuration on voltage, current and power output. Using a 0.1M KCl salt bridge with 6cm x 3cm copper and zinc electrodes, the cell output was measured. Furthermore, the effect of ZnSO₄ concentration (0.1M, 1M, 2M) was also tested. Rolled cells showed slightly higher voltage and current outputs, due to more effective electrode contact, however, both designs produced voltages below the theoretical 1.10V potential, due to current leakage, short circuits and lack of copper ions for cathodic reduction, increasing ZnSO₄ concentrations correlated with a decreasing cell voltage, aligning with predictions derived from the Nernst Equation. While the investigation generated reasonable results, deviations from theoretical values and measurement inconsistencies suggested experimental refinement is needed. The investigation provided insights into how cell geometry and electrolyte composition influence galvanic cell efficiency, providing insights into optimisation of electrochemical systems and contributing to sustainability in applications including energy storage and usage in electric vehicles and renewable energy storage^[1].

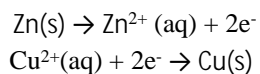
Keywords: galvanic cells, zinc-copper battery, rolled cell, flat-stacked cell, electrolyte concentration, power density, Nernst equation

1. Introduction

A galvanic cell is an electrochemical device which is used to produce electricity through a spontaneous redox reaction. The anode is composed of a compound with a low reduction potential, being readily oxidised to generate electrons which flow through an external wire to the cathode, facilitating the reduction of the cathode and generating an electrical current^[2]. The electrodes are submerged in an electrolyte solution, allowing the movement of ions, and maintaining neutrality within the cell. Batteries may contain one or more galvanic cells, converting chemical energy into electrical energy to fuel electric vehicles, phones, and off-grid renewable energy systems.

The application of a galvanic cell depends on the properties of the specific configuration utilised, including rolled, flat-stacked and half-cell designs. Rolled cells are very compact, and compared to flat stacked cells, they feature spiralled electrodes to increase the surface area for electron transfer, enhancing energy and power density^[3]. This design, seen in commercial formats like AA and 18650 batteries, offers scalability, thermal stability, and ease of production, making it ideal for EVs and portable electronics^[4], however, their stress concentrations may accelerate degradation. Flat-stacked cells, by contrast, use layered electrodes in a compact prismatic format, giving them better space utilisation and more uniform pressure distribution^[5]. While more challenging to manufacture due to alignment precision and contamination risks, flat-stacked designs deliver superior structural performance and offer better energy efficiency.

Zinc, being higher in the reactivity series compared to copper, displaces copper ions from the solution, depositing them as solid copper, leading to the oxidation of zinc. Hence, in a closed circuit, a current flows between the two electrodes, where zinc acts as the anode (supplying electrons) and copper acts as the cathode (consuming electrons)^[6], where the mass of the copper electrode increases. Copper and zinc electrodes, when immersed in electrolyte^[7], create an electrochemical cell which generates electrical energy through a redox reaction. This process involves the oxidation of zinc to form positive Zn^{2+} and $2e^-$, and the reduction of copper to form metallic copper from the consumption of electrons. The half-cell equations are shown below:



For the comparison of the rolled cell and flat cell, a 0.1M KCl solution was chosen as the electrolyte. To determine the impact of concentration on the cell output, the concentration of a $ZnSO_4$ electrolyte was changed under a flat cell configuration, and the output was recorded. The electrodes are responsible for influencing the power output of the cell (i.e. the rate at which chemical energy is transformed into electrical energy), and this is dependent on the surface area and material of the electrode. A larger surface area exposes a larger number of atoms to the electrolyte mixture, meaning the metallic atoms in the electrode can be oxidised into ions at a greater rate, thus increasing the power output^[8]. Furthermore, the reduction potential of a material will also influence the power. Anodes with a lower

reduction potential will be oxidised more efficiently, and when paired with a cathode with a higher reduction potential (easily reduced), the rate of the redox reaction is greater, increasing the efficiency and power output of the cell^[9].

Galvanic cells, while conventionally used as batteries, are now being used in the medical and environmental industries. Magnesium-based galvanic cells (MgG) are being used as a non-invasive tumour treatment as gas therapy. It involves micro-scale MgG rods being inserted into a tumour, with the Mg oxidised in the presence of water, forming both hydrogen gas and magnesium hydroxide^[10].



The hydrogen gas continuously produced induces mitochondrial dysfunction (by interfering with the electron transport chain) and impedes the maintenance of intracellular homeostasis. Furthermore, the Mg(OH)_2 can neutralise the acidic tumour environment. This helps to reduce toxicity on healthy cells and prevents the degradation of the extracellular matrix, thus preventing the spread of the tumour cells^[11].

2. Experimental Aim

To build and compare different types of Zinc-Copper galvanic cells, including flat and rolled cells, to compare their properties regarding voltage and current output and the ability to light up different coloured LEDs. To investigate the effect of electrolyte concentration on voltage output.

3. Materials & Methods

3.1 Materials

A zinc-copper electrode was employed for the galvanic cell design, the copper foil acting as the cathode and the zinc foil acting as the anode. Alligator clips and wires were used to close the circuit, connecting the electrodes to all other circuit components, including the AAA batteries and LEDs. Filter paper acted as the salt bridge within the galvanic cell with the use of a 0.1M KCl solution, maintaining neutrality within the cell and facilitating electron movement throughout the circuit. Different-coloured LEDs (green, blue, white, yellow, and red) were used to test the output of the galvanic cell design by changing the energy requirement from the cell. A multimeter was used to measure the voltage and current output of the cell. Finally, beakers were used to hold samples of the salt bridge solutions, the petri dish was used to soak the filter paper in the salt bridge solution, with tweezers were used to transport the soaked filter paper from the petri dish. Scissors were used to cut the sheets of copper and zinc into 3cm x 6cm strips, and tape was used to hold the rolled galvanic cell securely shut.

3.2 Method

The copper and zinc sheets were cut into 2 separate 3cm x 6cm strips. Two sheets of filter paper were then cut into 3cm x 6cm strips (as flush to the electrodes as possible to prevent the circuit from shorting). Approximately 30 mL of the 0.1M KCl solution was poured from the beaker into the petri dish, and one strip of filter paper was placed into the petri dish to soak. Tweezers were used to remove the filter paper from the petri dish, which was sandwiched between the copper and zinc electrodes. Tape was

then used to secure the stacked cell into a cylindrical rolled configuration (Figure 2). Separate alligator clips and wires were clamped onto each electrode, where the zinc electrode was connected to the negative (black) probe of the multimeter, and the copper electrode was connected to the positive (red) probe, creating a series circuit. The multimeter was switched to V mode, and the voltage was measured before being switched to mA mode to record the current. The alligator clip was disconnected from the positive terminal of the multimeter, and a new alligator clip was connected to the positive terminal of the green light bulb. Another wire with an alligator clip was used to close the circuit, connecting the negative terminal of the light bulb with the positive terminal of the multimeter. A battery was then added in series, and following this, a second battery was added in series, directly in contact with the previous battery. The voltage and current were then recorded. The green light bulb was removed from the circuit and replaced with the blue light bulb, again measuring the voltage and current. This step was repeated for the white, yellow and red light bulbs, recording each voltage.

The second strip of filter paper was soaked in the petri dish with the 0.1M KCl solution, and the filter paper was placed between the second zinc and copper strips, creating a flat cell (Figure 2). An alligator clip was used to connect the positive probe of the multimeter to the copper electrode, while another wire and alligator clip were used to connect the zinc electrode to the negative multimeter probe. The initial voltage and current were then recorded. The green light bulb was then connected in series, disconnecting the alligator clip from the positive multimeter terminal, and connecting it to the positive terminal of the green light bulb before closing the circuit by using a new wire to connect the negative terminal of the light bulb to the positive multimeter probe. 2 batteries were added to the circuit in series. The green light was replaced with the blue, white, yellow then red light bulb, testing its ability to light up each colour.

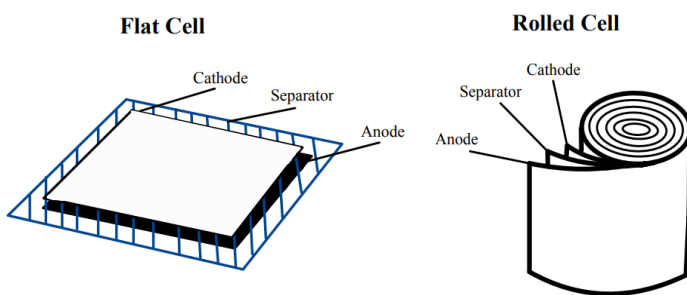


Figure 2. Flat-stacked and rolled cell configurations

4. Discussion

Our investigation compared the output and efficiency of a rolled and flat galvanic cell, as well as the effect of ZnSO_4 electrolyte concentration on cell output. Both cells contained a copper and zinc electrode, with a 0.1M KCl solution used as a salt bridge and separator. The standard reduction potentials for zinc and copper, as shown in Table 4, are -0.76V and 0.34V, respectively. This indicates that the copper electrode will undergo reduction, acting as the cathode. To obtain the standard potential of the cell, the reduction potential of the anode is subtracted from that of the cathode^[13], as demonstrated in Equation 1. This yields an

3.3 List of Equations Applied to Raw Data Analysis

The formula used to calculate the standard potential of the cell is shown in Equation 1, where E° represents the standard reduction potential of the cathode and anode. However, galvanic cells are often operated at non-standard conditions, where the Nernst Equation may be used (Equation 2). This takes into account factors such as temperature, pressure and the reaction quotient^[12].

Equation 1 - Calculating the standard reduction potential of a full cell:

$$E^\circ = E^\circ(\text{cathode}) - E^\circ(\text{anode})$$

Equation 2 - The Nernst Equation:

$$E = E^\circ - \frac{RT}{nF} \ln Q$$

E° = Reduction potential of the cell, R = Ideal gas constant (8.314 J K⁻¹mol⁻¹), T = Temperature (K) and n = number of electrons transferred.

Equation 3 - Ohm's Law:

Furthermore, Ohm's Law is discussed in the discussion to compare the relationship between the voltage (V), current (I) and resistance (R) within the circuit, where voltage is in volts (V), current is in amperes (A), and resistance is given in Ohms (Ω). This is rearranged as shown below to distinctly compare the current changes involving voltage and resistance.

$$V = IR$$

This is then rearranged to: $I = \frac{V}{R}$

The power within the cells is also studied, where power (Watts) is shown in Equation 4, with V representing the voltage (V) and I representing the Current (A).

Equation 4 - Power (W):

$$P = VI$$

To calculate the overall voltage within a series circuit, the voltage of each power source can be added, providing the final voltage as shown in Equation 5.

Equation 5 - Voltage in Series:

$$V = V_1 + V_2 + \dots + V_n$$

overall standard reduction potential of 1.10V for the entire cell. Table 1 shows that the voltage output for the flat stacked cell was 0.6659V, while Table 2 shows that for the rolled cell, the output was 0.7462V. This indicates a loss of 0.4341V (or an efficiency of 60.5%) for the flat stacked cell, and a loss of 0.3538V (or an efficiency of 67.84%) compared to the theoretical potential at standard conditions.

Overall, the output was much smaller than the predicted voltage output of 1.10V (Figure 4), likely due to the leakage of voltage

and current because of electrolyte leakage or unintended contact of electrodes, leading to a short circuit^[14], as well as unintended contact of the electrodes due to faulty use of the separators. Additionally, another cause of shorts is the production of dendrites, which are tiny metallic projections that extend across and pierce the separator, leading to electrode contact^[15].

Due to shorts and the leakage of current, differing results were observed between the rolled and flat cell batteries. For the flat cell, a voltage reading of 0.6659 V was taken, lower than the 0.7462V value taken for the rolled cell. The configuration of the cell was likely the reason for the varied data. The flat-stacked cell has great contact between the electrodes across the whole surface, facilitating the exchange of electrons, and hence leading to a greater voltage^[16]. However, as seen in *Table 1*, the rolled cell can reduce the contact and uniformity of electron and ion transfer between the electrodes, leading to reduced voltage and current^[17]. Furthermore, both cells had voltages significantly lower than the theoretical standard potential of 1.10 V, indicating sources of error, including the absence of a Cu²⁺ or Zn²⁺ electrolyte. Instead, a 0.1M KCl solution was used as the electrolyte, which doesn't include Cu²⁺ or Zn²⁺, thus inhibiting the reaction as the copper cathode requires Cu²⁺ ions to be able to accept electrons and act as the reducing agent.

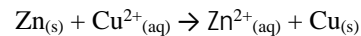
As shown in *Table 1*, the voltage of the circuits with no batteries was significantly lower than that of the circuits containing 2 batteries. For example, in the flat cell, the voltage with no battery was 0.6659V, while that of the rolled cell was 0.7462. This indicates that a voltage was successfully generated, despite being much lower than the predicted value of 1.10V. When 2 batteries were supplied to the circuit, the voltage of the flat cell circuit was 3.9667V while the voltage of the rolled cell circuit was 4.0321V. Adding more batteries in series directly increases the voltage because batteries themselves contain voltage, and the final voltage of the circuit is the sum of the voltage in each component of the circuit, as demonstrated in *Equation 5*. Furthermore, as a higher voltage was supplied, the current of both cells also increased (from 1.621 mA to 25.874mA in the flat cell and from 1.731mA to 26.635mA in the rolled cell), resulting from the direct proportionality of voltage and current, as demonstrated in *Equation 3*. A higher voltage provides a larger force to push a constant number of electrons through a circuit, leading to the increased current observed (Figure 3) ^[18].

Furthermore, *Table 2* demonstrates that in both cells, no light bulbs lit up when supplied with the voltage from only the galvanic cell; however, when the 2 batteries were added in series, all light bulbs lit up in both cells. This is because different amounts of energy are required to light up each bulb, with the red and yellow light bulbs requiring the lowest voltage to light up, at just 2 - 2.2 V. In contrast, the white, blue, and green light bulbs required the largest voltage to light up, between 3 - 3.2 V. Hence, the initial voltage of the flat and rolled cells (0.6659V and 0.7462V, respectively) didn't provide enough energy to light up the bulb, yet after adding the batteries, the voltage exceeded 3.2V in both circuits, meaning an adequate voltage was reached to light each bulb in both circuits.

Moreover, *Table 4* demonstrates that the voltage output of the Zn-Cu flat-stacked cell decreases with increasing ZnSO₄

concentration. Specifically, when the concentration of ZnSO₄ is 0.1 mol/L, the voltage is 0.958V, yet at 1.0 mol/L, this reduces to 0.8740 V, and finally, at 2.0 mol/L, the voltage drops further to 0.8505 V. The results obtained support the theoretical prediction given by the Nernst Equation (*Equation 2*), which accounts for non-standard conditions and the effect of changing ion concentrations on cell potential.

For the zinc-copper cell, the full redox reaction is:



Under this reaction, the reaction quotient is:

$$Q = \frac{[\text{Zn}^{2+}]}{[\text{Cu}^{2+}]}$$

Assuming a constant Cu²⁺ concentration (1.0 mol/L), the Nernst Equation simplifies to a dependence on the Zn²⁺ ion concentration, which is equal to the concentration of the ZnSO₄ electrolyte used. Therefore, substituting this into the Nernst equation gives us:

$$E = E^{\circ} - \frac{RT}{nF} \ln [\text{ZnSO}_4]$$

This relationship shows that voltage decreases logarithmically as ZnSO₄ concentration increases, which is shown in *Figure 5*, and can be expressed in a proportional form equation as:

$$E \propto -\log[\text{ZnSO}_4]$$

This relationship reinforces the theoretical prediction that higher Zn²⁺ concentrations increase the reaction quotient (Q), therefore reducing the cell potential. A comparison between the experimentally observed voltages and the cell potentials computed using the Nernst equation is made in order to verify the theoretical model. At 298 K, the Nernst equation reduces to:

$$E = 1.10 - 0.01285 \ln [\text{ZnSO}_4]$$

$$E^{\circ} = 1.10 \text{ V}, R = 8.314 \text{ J K}^{-1} \text{ mol}^{-1}, T = 298 \text{ K}, n = 2, F = 96,485 \text{ C mol}^{-1}$$

Table 4 compares the theoretical voltages obtained using this equation with the observed experimental data. The observed voltages are consistently lower than the theoretical predictions derived from the Nernst equation. This disparity can be explained by several related experimental constraints and not ideal circumstances that are typical of real-world electrochemical systems. One major factor is internal resistance arising from the flat-stacked cell design. Although this configuration allows uniform surface contact between electrodes and electrolyte, resistance still arises from ionic drag in solution, imperfect electrode-wire connections, and contact resistance at the metal-clip interface^[19]. These losses reduce the effective voltage when measured using the multimeter. Inconsistent placement of alligator clips on the flat electrodes also contributes to inconsistent electrical contact. Subsequently, another significant factor is the absence of Cu²⁺ ions for the cathode half-cell reaction. Theoretically, Cu²⁺ is reduced to Cu_(s) at the cathode. However, in this experiment, only ZnSO₄ was used as the electrolyte, meaning that no Cu²⁺ ions were present to accept

electrons at the copper electrode. Therefore, the cathode acts as a passive conductor rather than an active reduction site, suppressing the full redox process and lowering the cell potential^[20]. Finally, short circuits and measurement inconsistencies also contribute to the voltage drop. In the experimental configuration, there is a risk that the zinc and copper sheets make physical contact, bypassing the electrolyte and creating a low-resistance path. This short-circuiting can discharge the cell prematurely and skew the voltage readings^[21].

The applications of rolled or flat-celled batteries are dependent on their efficiency, sustainability, and cost, regarding the specific application. The simple design of rolled cells supports automated manufacturing processes, leading to efficient production, low costs, and a high degree of uniformity.^[22] The standardised manufacturing of rolled cell batteries leads to more efficient use of materials, lower energy consumption and streamlined recycling processes^[23], resulting in a lower carbon footprint and a more sustainable battery configuration. Rolled cells are the cell configuration typically used in standard consumer batteries available in supermarkets. Conversely, flat-stacked cell batteries optimally use available space, enhancing energy density, making the configuration suited to applications such as smartphones and other portable electronics^[24].

Overall, while the aim was fulfilled and the effects of cell type and electrolyte concentration were successfully related to the cell output (voltage and current), the investigation was invalid due to the unreliability and inaccuracy of the results acquired. Rolled cells resulted in a larger output for both the voltage and current. In circuits with no batteries, both circuits were unable to light up any of the light bulbs; however, when 2 batteries were added in series, all light bulbs were lit up in both circuits. Furthermore, a larger concentration of the electrolyte resulted in a lower voltage, as demonstrated in *Table 3*. However, the results significantly deviated from the theoretical value of 1.10V, indicating a significant source of error in our method, which would require more testing to determine the specific cause. Furthermore, due to the discrepancies between the theoretical value and the experimental value, as well as the inconsistency in results across multiple trials, our experiment is unreliable. To improve our data, more tests should be done in order to identify if the results are consistent across trials. Furthermore, testing cells which are stacked with multiple layers would have allowed conclusions to be made about the impact of surface area on the output of the cells, along with the effect of the number of layers on the ability to compact cells for storage, which could be related to the applications of cells.

5. Conclusion

Ultimately, the investigation determined that, in comparison to the flat cell, the rolled cell yielded a higher voltage and current for the same electrode surface area. For each series circuit, the voltage with no batteries was 0.6659V and 0.7462V for the flat and rolled cell, respectively. This was likely due to the uniformity of electron and ion transfer. Furthermore, increasing the concentration of the electrolyte decreased the voltage of the cell, as shown in *Table 4*, where the voltage of the 0.1M ZnSO₄ was 0.958 V compared to 0.8505 V for the 2M ZnSO₄. The effect

of concentration is explained by the Nernst Equation (Equation2), whereby increasing the concentration of products compared to the reagents will reduce the voltage. Despite achieving the aim of the investigation, our investigation was invalid due to unreliability and significant deviations from the theoretical values. To improve our investigation, the number of trials should be increased to test for consistency, and the surface area should be increased by stacking more electrodes to investigate the effect of surface area on electron transfer and power density. Irrespective, future research could explore the use of sustainable or biodegradable electrode and electrolyte materials to minimise the environmental impact of galvanic cells, making electrochemical cells more viable for green energy storage solutions^[25]. Additionally, optimising cell geometry and reducing internal resistance could contribute to the development of more efficient, compact energy systems for both portable electronics and renewable energy applications.

Authorship Contribution Statement

Emily Sewell co-wrote the abstract, introduction, discussion, and conclusion, wrote the materials & methods and contributed to the discussion. Manas Srinivas co-wrote the abstract, introduction, materials & methods, discussion, conclusion, and conducted the literature review. Lucas Sidney compiled the data tables and processed experimental results. Jacinta Wilkin contributed to drafting the discussion, reviewed and edited the full manuscript, and contributed to the final referencing. Bryan Law analysed trends in voltage and electrolyte concentration and wrote the equations and derivations. Dr. Thomas Whittle designed the experiment. Dr. David Alam facilitated project resources and guidance on conceptual direction. Dr. Gobinath Rajarathnam ideated conceptual direction, research and writing guiding frameworks, and direct project supervision.

Acknowledgements

Along with the use of generative AI, Group 7's (Madison Louey, Melissa Marshall, Jun Wei Wong, Audrey Wang, Alan Lun) raw current and voltage data, compared to the concentration of ZnSO₄, as seen in *Table 3*, were incorporated to determine and evaluate the effect of concentration on voltage.

References

1. Jeon, B.-J., Lee, Y.-H. & Jeong, K.-M. Unveiling the Impact of Electrode Curvature on N/P Ratio Variations in Cylindrical Lithium-ion Batteries. *Energy storage materials* 104117–104117 (2025) doi:<https://doi.org/10.1016/j.ensm.2025.104117>.
2. Janzen, A. F. Photoelectrochemistry II - The Photogalvanic Cell *Elsevier eBooks* 923–937 (1979) doi:<https://doi.org/10.1016/b978-0-08-024744-1.50036-x.3>.
- Bhattacharjya, D., Carriazo, D., Ajuria, J. & Villaverde, A. Study of electrode processing and cell assembly for the optimised performance of supercapacitor in pouch cell configuration. *Journal of Power Sources* 439, 227106 (2019).
3. Zhu, J. *et al.* End-of-life or second-life options for retired electric vehicle batteries. *Cell Reports Physical Science* 2, 100537–100537 (2021).

4. Saber, N., Richter, C. P. & Runar Unnþorsson. Review of Thermal Management Techniques for Prismatic Li-Ion Batteries. *Energies* 18, 492–492 (2025).

5. Electrochemistry: Galvanic Cells and the Nernst Equation. *Chemcollective.org* https://chemcollective.org/chem/electrochem/step2_cell.php#:~:text=In%20the%20movie%20on%20the,Tap%20to%20unmute (2021).

6. Nazarian-Samani, M., Alidokht, S. A., Heloise Therien-Aubin & Zhang, L. Mechanical structure design: A survey on modern triboelectric nanogenerators. *Applied Energy* 391, 125918–125918 (2025).

7. Moradi, H. G., Mahdavi, M. A., Reza Gheshlaghi & Mozhdeh Dehghanian. Electrochemical evaluation of the effect of anode to cathode surface area ratio on power generation in air-cathode microbial fuel cells. *Journal of Applied Electrochemistry* 53, 2433–2442 (2023).

8. JEI. Analysis of reduction potentials to determine the most efficient metals for electrochemical cell alternatives | Journal of Emerging Investigators. *Emerginginvestigators.org* <https://emerginginvestigators.org/articles/19-088> (2020).

9. Yang, N. et al. Magnesium galvanic cells produce hydrogen and modulate the tumour microenvironment to inhibit cancer growth. *Nature Communications* 13, (2022).

10. Alberts, B. et al. The Mitochondrion. *Nih.gov* <https://www.ncbi.nlm.nih.gov/books/NBK26894/#:~:text=The%20electrochemical%20proton%20gradient%20across,enzyme%20ATP%20synthase%2C%20mentioned%20previously>. (2025).

11. Feiner, A.-S. & McEvoy, A. J. The Nernst Equation. *Journal of Chemical Education* 71, 493 (1994).

12. Waag, W. & Sauer, D. U. SECONDARY BATTERIES – LEAD-ACID SYSTEMS | State-of-Charge/Health. Elsevier eBooks 793–804 (2009) doi:<https://doi.org/10.1016/b978-044452745-5.00149-0>.

13. Shea, H. R. et al. Effects of Electrical Leakage Currents on MEMS Reliability and Performance. *IEEE Transactions on Device and Materials Reliability* 4, 198–207 (2004).

14. Peng, J. et al. Electrolyte effects on the electrochemical performance of microemulsions. *Electrochimica Acta* 393, 139048–139048 (2021).

15. Timurkutluk, B., Timurkutluk, C., Mat, M. D. & Kaplan, Y. A review on cell/stack designs for high-performance solid oxide fuel cells. *Renewable and Sustainable Energy Reviews* 56, 1101–1121 (2016).

16. Willert, A., Voigt, S., Zschau, T. & Zichner, R. Printed Primary Battery in a Rolled-Up Form Factor. *Designs* 8, 62 (2024).

17. Licari, J. J. & Swanson, D. W. Functions and theory of adhesives. Elsevier eBooks 35–74 (2011) doi:<https://doi.org/10.1016/b978-1-4377-7889-2.10002-6>.

18. Moral, C. G. et al. Battery Internal Resistance Estimation Using a Battery Balancing System Based on Switched Capacitors. *IEEE Transactions on Industry Applications* 56, 5363–5374 (2020).

19. Zavalis, T. G., Behm, M. & Lindbergh, G. Investigation of Short-Circuit Scenarios in a Lithium-Ion Battery Cell. *Journal of The Electrochemical Society* 159, A848–A859 (2011).

20. Zavalis, T. G., Behm, M. & Lindbergh, G. Investigation of Short-Circuit Scenarios in a Lithium-Ion Battery Cell. *Journal of The Electrochemical Society* 159, A848–A859 (2012).

21. Schröder, R., Aydemir, M. & Seliger, G. Comparatively Assessing different Shapes of Lithium-ion Battery Cells. *Procedia Manufacturing* 8, 104–111 (2017).

22. Wilke, C., Kaas, A. & Urs Alexander Peuker. Influence of the Cell Type on the Physical Processes of the Mechanical Recycling of Automotive Lithium-Ion Batteries. *Metals* 13, 1901–1901 (2023).

23. Sabri Baazouzi et al. Design, Properties, and Manufacturing of Cylindrical Li-Ion Battery Cells—A Generic Overview. *Batteries* 9, 309–309 (2023).

24. Ayat Gharehghani et al. Progress in battery thermal management systems technologies for electric vehicles. *Renewable and Sustainable Energy Reviews* 202, 114654–114654 (2024).

Appendix

Table 1. Raw data reflecting the flat-stacked and rolled cell voltage, current, and power, with one battery and two batteries.

Battery Type	Voltage (V)		Current (mA)		Power (mW)	
	No Battery	With 2 Batteries	No Battery	With 2 Batteries	No Battery	With 2 Batteries
Flat-stacked battery cell	0.6659	3.9667	1.621	25.874	1.079	102.7
Rolled battery cell	0.7462	4.0321	1.731	26.635	1.2917	107.39

Table 2. Raw data reflecting LED colour, corresponding wavelength, required voltage and light-up test.

Flat-Stacked and Rolled Battery Layout	LED Colour	Wavelength (nm)	Required Voltage (V)	Activated	
No Battery	Red	625-750	2.0 - 2.2	No	
	Yellow	565-590			
	White	400-700			
	Blue	450-485			
	Green	500-565			
2 Batteries	Red	625-750	2.0 - 2.2	Yes	
	Yellow	565-590			
	White	400-700	3.0 - 3.2		
	Blue	450-485			
	Green	500-565			

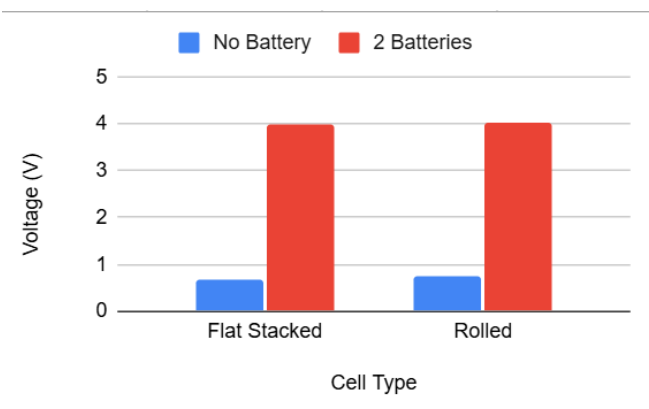


Figure 3 - The voltage in a flat cell and a rolled cell with no battery compared to 2 batteries.

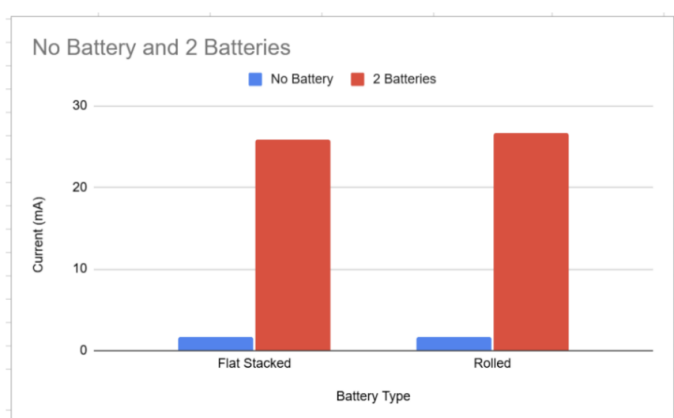


Figure 4 - The current in a flat cell and a rolled cell with a battery compared to 2 batteries.

Table 3. Raw data reflecting changes in the voltage, current and power compared to the concentration of $ZnSO_4$

Concentration of $ZnSO_4$ (mol/L)	Voltage (V)	Current (mA)	Power (mW)
0.1	0.958	25.874	24.787
1	0.874	23.724	20.735
2	0.8505	22.851	19.435

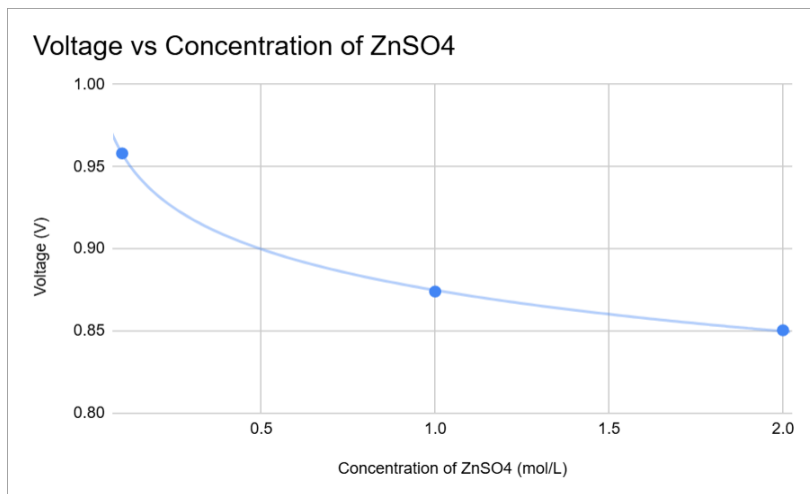


Figure 5 - The concentration of $ZnSO_4$ electrolyte compared to the voltage produced

Table 4. The difference between the theoretical voltage and experimental voltage at different $ZnSO_4$ concentrations

$ZnSO_4$ (mol/L)	$\ln[ZnSO_4]$	Theoretical Voltage (V)	Observed Voltage (V)	% Difference
0.1	-2.3026	1.1296	0.9580	15.2%
1.0	0.0000	1.1000	0.8740	20.5%
2.0	0.6931	1.0911	0.8505	22.0%